Biological smart sensing strategies in weakly electric fish

Mark E. Nelson*

*Department of Molecular & Integrative Physiology, Neuroscience Program, Beckman Institute,
University of Illinois at Urbana-Champaign, Urbana, IL 61801, USA*

Abstract. Biological sensory systems continuously monitor and analyze changes in real-world environments that are relevant to an animal's specific behavioral needs and goals. Understanding the sensory mechanisms and information processing principles that biological systems utilize for efficient sensory data acquisition may provide useful guidance for the design of smart-sensing systems in engineering applications. Weakly electric fish, which use self-generated electrical energy to actively sense their environment, provide an excellent model system for studying biological principles of sensory data acquisition. The electrosensory system enables these fish to hunt and navigate at night without the use of visual cues. To achieve reliable, real-time task performance, the electrosensory system implements a number of smart sensing strategies, including efficient stimulus encoding, multi-scale virtual sensor arrays, task-dependent filtering and online subtraction of sensory expectation.

Keywords: adaptive filtering; bio-inspired; multi-scale; neurobiology; sensory system.

1. Introduction

All animals are faced with the challenging task of extracting useful information about their environment from the barrage of stimuli impinging on their sensory receptors. The vertebrate nervous system typically processes data from millions of receptors that are continuously monitoring auditory, visual, chemical, tactile, thermal, and other sensory stimuli. Of all the information contained in this rich, multi-channel, multi-modal data stream, only a small fraction is relevant to the animal's particular behavioral needs at any given point in time. Animals therefore use a variety of strategies to encode, filter, and process the incoming data stream so as to enhance signals of behavioral relevance and suppress irrelevant background signals. Engineers are faced with similar data acquisition and processing challenges when designing smart sensing systems for real-world engineering applications.

Certain freshwater fishes from South America and Africa use millivolt-level, self-generated electrical discharges to actively monitor their environment (Nelson and MacIver 2006). These so-called weakly electric fish generate electric fields using a specialized electric organ located in the tail region of the fish. The temporal properties of the electric organ discharge (*EOD*) can be qualitatively assessed by placing a pair of wires in the water near the fish and listening to the *EOD* signal on an audio monitor. The *EOD* patterns of weakly electric fish fall into two broad

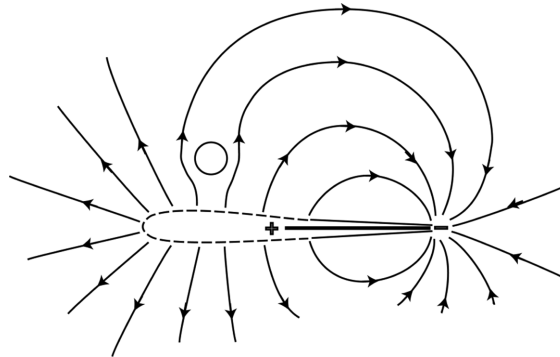*Corresponding Author, Professor, E-mail: m-nelson@illinois.edu

Fig. 1 Physical basis of active electrolocation. The electric organ (horizontal black bar) gives rise to a dipolar field. Electric current follows the field lines (solid with arrows). A non-conducting object (circle) perturbs the flow of electric current, causing a local decrease in current density, which translates into a decrease in the voltage across the skin near the object. Redrawn from Heiligenberg (1977)

categories. Pulse-type fish generate brief discharges separated by significantly longer gaps, such that the audio output sounds like a series of clicks. Wave-type electric fish generate *EOD*s with little or no gap between successive discharges, resulting in a quasi-periodic signal that sounds like a tone or hum.

The electric field has an approximately dipolar spatial structure (Knudsen 1975). Objects that differ in electrical impedance from the surrounding water (such as rocks, plants, and prey) perturb the flow of electric current near the fish. For example, a non-conducting object near the fish would block the flow of electrical current, causing the current lines to flow around the object as shown in Fig. 1. These perturbations give rise to changes in the local potential difference across the skin of the fish, referred to as the transdermal voltage (Nelson 2005). The transdermal voltage changes are monitored by specialized sense organs distributed over the skin of the fish. The active electrosensory system allows the fish to detect, identify and localize objects in its environment even in complete darkness. This capability is called electrolocation, in analogy to the echolocation capability of bats and dolphins.

2. Stimulus encoding

The body of the fish is covered with thousands of small sensory pores, each of which acts like a miniature voltmeter and converts the local transdermal voltage into a sequence of nerve spikes. The conversion of the stimulus into a sequence nerve spikes is called stimulus encoding. In South American fish with a wave-type *EOD*, the encoding of stimulus amplitude is carried out by a particular subclass of afferent nerve fibers called probability-coding (*P*-type) afferents. These nerve fibers fire irregularly, with an average rate of about one spike for every three *EOD* cycles. Changes in the amplitude of the transdermal voltage, which are typically less than 10% for naturalistic stimuli, are encoded as changes in the firing probability per *EOD* cycle. So, for example, a typical *P*-type afferent might have a baseline per-cycle firing probability of 0.33, and this probability might vary between 0.30 and 0.36 depending on the local stimulus intensity. A representative *P*-type afferent spike train is shown in Fig. 2(a).
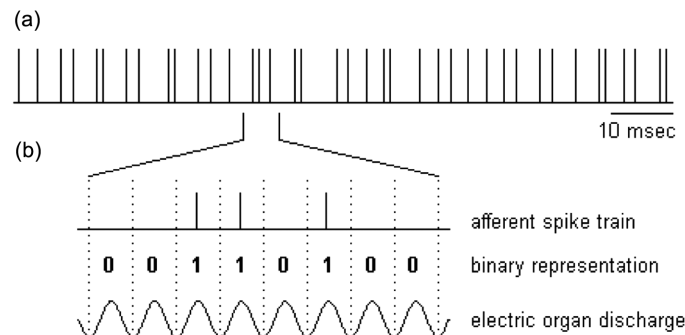
Fig. 2 Sensory encoding by *P*-type electrosensory afferents. (a) Representative *P*-type afferent spike train recorded from the brown ghost knifefish, *Apteronotus leptorhynchus* (Ratnam and Nelson 2000). Scale bar: 10 msec and (b) enlargement of a portion of the data record illustrating a binary representation of the spike train data as a sequence of 1s and 0s, based on whether or not a spike is present on each cycle of the sinusoidal electric organ discharge (*EOD*) waveform

2.1 Sampling rate and resolution

Because P-type afferents never fire more than one spike per *EOD* cycle, the firing pattern can be represented as a sequence of ones and zeros, as illustrated in Fig. 2(b). The effective sampling rate for the binary sequence is the fish's *EOD* frequency, which can vary between about 200 and 1200 Hz, depending on the species. The brown ghost knifefish *Apteronotus leptorhynchus*, the subject of many of our empirical studies, has a typical *EOD* frequency near 1000 Hz. In this species each electroreceptor sense organ can be thought of as a sort of 1-bit analog-to-digital converter (*ADC*) operating at a sampling frequency of 1 kHz.

This sampling frequency is much higher than might be expected based on the demands of the electrolocation task. It turns out that electrolocation signals are predominantly low frequency with a bandwidth less than about 10 Hz (Nelson and MacIver 1999). The Nyquist rate, which is twice the signal bandwidth, is therefore on the order of 20 Hz. By operating at 1000 Hz, the fish is therefore oversampling by a factor of about 50 relative to the Nyquist rate. Oversampling allows the fish to increase the effective resolution of the analog-to-digital conversion process associated with converting stimuli into spike trains. This can be illustrated by considering a simple decoding scheme that interprets the binary spike train sequence in blocks of 50 bits, with the blocks being sampled at 20 Hz. Using a spike-count-based coding scheme, the data value for each 50-bit "word" can vary between zero (no spikes) and 50 (one spike on every *EOD* cycle). In this simple scheme, the original 1-bit data stream sampled at 1 kHz can be reinterpreted as a 5.6-bit ($\log_2 50$) data stream sampled at 20 Hz (the Nyquist rate). The fish undoubtedly uses a more sophisticated decoding strategy, but this provides an estimate of the intrinsic sensor resolution for low frequency signals. The roughly 6-bit resolution available to the fish is rather crude when compared to the more typical 12-16 bit resolution of *ADCs* used in many engineering applications.

2.2 Intrinsic sensor noise

To assess how reliably signals of interest can be detected by the fish's electrosensors, it is necessary to compare the expected signal size with the intrinsic sensor noise. Recall that changes in firing rate

associated with naturalistic stimuli are at most about ±10% of the baseline transdermal voltage. *P*-type afferents tend to fire on about 1/3 of the *EOD* cycles, so a 50-bit "word" would typically contain about 17 spikes, with some random variation. A 10% signal variation in signal strength would translate into a change of about ±2 spikes around the mean of 17 spikes.

Under baseline conditions with no target present (stimulus = 0) there will still be random fluctuations in the spike count per 50-bit word. If spikes were generated independently on each *EOD* cycle with a probability *p* of 1/3, then spike encoding would be described by a binomial process. In this case, the spike train could be envisioned as being generated by tossing a weighted coin where heads corresponds to a one (spike) and tails corresponds to zero (no spike). For a binomial process with sample-size *n* and probability *p*, the expected spike count is np and the standard deviation is $\sqrt{np(1-p)}$; for $n = 50$ and $p = 1/3$ this corresponds to a mean spike count of 16.7 and a standard deviation of 3.3 spikes. If afferent spike trains were indeed binomial, then intrinsic fluctuations in spike count (±3.3 spikes) would be larger than the maximum expected signal size (±2 spikes). This would correspond to a signal-to-noise ratio of less than one and would pose a significant signal processing challenge. In reality, *P*-type afferent spike trains are more regular than a binomial process due to the correlation structure arising from dynamic properties of the spike generating mechanism (Ratnam and Nelson 2000, Brandman and Nelson 2002). The actual spike count variability in a 50-bin window has been measured empirically to be on the order of ±1 spike (Ratnam and Nelson 2000). Still this means that the signal-to-noise ratio for individual electrosensory afferents is rather low, typically less than two. Based on these observations, we conclude that the fish's electrosensory system operates with rather noisy, low resolution devices.

2.3 Stimulus filtering and whitening

In addition to intrinsic sensor noise, the electrosensory system also has to contend with extrinsic sources of noise from the environment. To reduce the impact of extrinsic noise, the system implements several stimulus filtering strategies during the encoding process. For example, the electroreceptive sensory cells are tuned in the frequency domain to respond best to frequency components of the input near the fish's own *EOD* frequency (Hopkins 1976). This tuning to the *EOD* carrier frequency improves the signal-to-noise ratio by filtering out environmental background noise in frequency bands that are unrelated to active electrolocation.

In addition to band-pass filtering the stimulus around the *EOD* carrier frequency (typically around 1 kHz), a second type of filtering takes place which is related to the frequency components of the amplitude modulation (*AM*) signal that arises as a target moves past the sensor array. The *AM* frequencies relevant to electrolocation signals are predominantly low frequency with a bandwidth less than about 10 Hz (Nelson and MacIver 1999). Within this range, fast-moving targets will cause higher-frequency *AM*s compared to distant, slow-moving targets. Electroreceptors act as high-pass filters in the *AM* frequency domain, giving the strongest response to high-frequency *AM* components of the signal (Nelson *et al.* 1997). If a target remains stationary relative to the fish, afferent activity gradually adapts back to baseline firing with a multi-scale relaxation time course (Xu *et al.* 1996). The high-pass *AM* filtering properties and adaptation characteristics reflect the fact that *changes* in the local transdermal voltage carry more behaviorally relevant information than the absolute magnitude of the transdermal potential.

The *AM* frequency spectrum for naturalistic electrosensory background noise has an approximate 1/*f* dependence, as has been observed in many natural systems. The high-pass *AM* characteristics of

P-type afferents appear to be complementary to the low-frequency bias of the 1/*f* background noise. In experiments where naturalistic noise is used as a stimulus, the spike trains recorded from *P*-type afferent have a nearly flat power spectrum. This 'whitening' of the input by high-pass filtering removes low frequency temporal correlations from the input data stream prior to processing by the central nervous system. From a statistical signal-processing perspective, whitening of the input signal is expected to be one of the first steps in optimal signal detection and estimation (Kay 1993).

3. Electrosensory images

In the context of electrolocation, the fish is interested in more than analyzing transdermal voltages at individual points on the body surface as conveyed by single sensors. The fish must combine information from multiple sensors in order to assess behaviorally relevant properties like target size, distance, location and composition. This is accomplished by analyzing dynamic electrosensory "images" on the body surface. These images correspond to changes in transdermal voltage across the electroreceptor surface of the fish's skin, just as visual images correspond to changes in light intensity across the photoreceptor surface of the retina of the eye.

Electrosensory images can be envisioned as bright and dark patches moving across the fish's body surface. When the fish is swimming near a non-conductive object, like a rock, the object will cause a local decrease in electric current density and thus cast a sort of electrosensory shadow on the surface of the fish as it moves past the object. A highly conductive object, like a metal sphere, would cause a local increase in current density and give rise to an electrosensory bright spot on the receptor surface. Since there is no functional equivalent to the lens of the eye, electrosensory images are blurred. The amount of blurring increases with target distance. As a general rule, the electrosensory image of a small target has a 2D Gaussian-like profile on the receptor surface with an image width (full-width at half-maximum) that is about equal to the distance of the target from the receptor surface (Chen *et al.* 2005). So a small target, like a piece of food, that is located a few centimeters from the body surface will excite the electroreceptors in a roughly circular patch of skin with a diameter of a few centimeters. Weakly electric fish are typically 10-20 cm in length, so the electrosensory image of a single target often excites a significant fraction of the electroreceptor population.

Another important property of electrosensory images is that the peak intensity of the image drops off rapidly with increasing target distance. At large distances of more than a body length, the peak intensity falls approximately as d^{-4}, where d is the distance from the midline of the body (Chen *et al.* 2005). Because of this rapid drop in signal strength with distance, weak signals from distant targets will often fall below the noise floor of the system making them undetectable. Thus the active electric sense is a short-range sense. It has an effective working range of a few centimeters for detecting small prey and about one body length (10-20 cm) for detecting larger objects like rocks and plants.

3.1 Spatial sampling

In Section 2 we saw that the fish oversamples electrosensory stimuli in the time domain. Oversampling also occurs in the spatial domain. The body of the fish is covered with approximately 15,000 electroreceptor organs. This corresponds to a sensor density on the trunk of the fish of approximately 3 sensors per square millimeter (Carr *et al.* 1982). If we consider the electrosensory image of a small target located 1 cm from the fish, the width of the Gaussian image on the skin
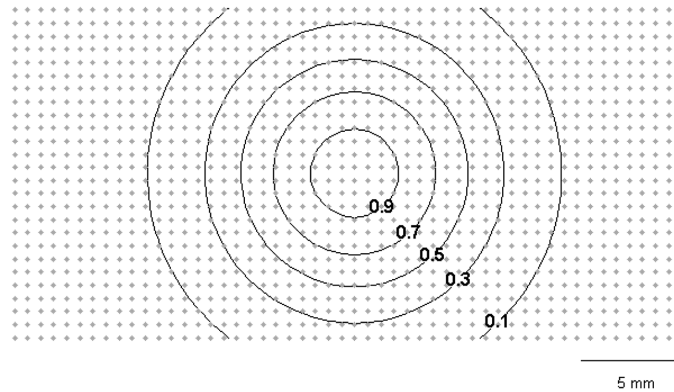
Fig. 3 An electrosensory image profile superimposed on an idealized sensor array. This figure illustrates a 30 mm × 15 mm patch of skin containing approximately 1350 electroreceptors (small dots), corresponding to an electroreceptor density of 3 sensors/mm^2 as found on the trunk of the fish. Iso-intensity contours represent the normalized transdermal voltage modulation across the surface of the receptor array. The image has a full width at half maximum (FWHM) of 10 mm, which would correspond to a small electrolocation target located approximately 10 mm from the surface of the skin. Each sensor in the array independently encodes the local transdermal voltage modulation into a spike train similar to that shown in Fig. 2. Scale bar: 5 mm

surface would also be about 1 cm. There would be several hundred electroreceptors falling within the region activated by the target, as illustrated in Fig. 3. It may seem somewhat surprising that the fish should use so many sensors to sample blurred electrosensory images that contains only low spatial frequencies. But the strategy of using a very large number of sensors makes is understandable when we consider that each individual sensor is relatively noisy and encodes information with relatively low resolution, as discussed in Section 2 above. In order to reliably detect weak signals and to estimate target parameters (e.g., size, speed, distance) from electrosensory images, the fish relies on the pooling of information from a large number of rather noisy sensors. The electrosensory array provides data samples from many more spatial locations than would be necessary based solely on the spatial frequency content of the images.

4. Central processing

The next stage of electrosensory information processing takes place in the central nervous system in a structure called the electrosensory lateral line lobe (*ELL*). The *ELL* is the sole recipient of electrosensory primary afferent input and thus all electrosensory information needed to support electrolocation passes through this structure. A key organizational feature of the *ELL* is that it contains multiple topographically organized maps of the fish's body surface (Maler 2009, Shumway 1989a). Electrosensory images that appear as spatially localized voltage perturbations on the fish's skin are transformed into spatially localized patterns of neural activity in parallel *ELL* maps (Fig. 4).

4.1 Multi-scale virtual sensor arrays

As shown in Fig. 4(a), the *ELL* of wave-type electric fish contains four subdivisions, each with its
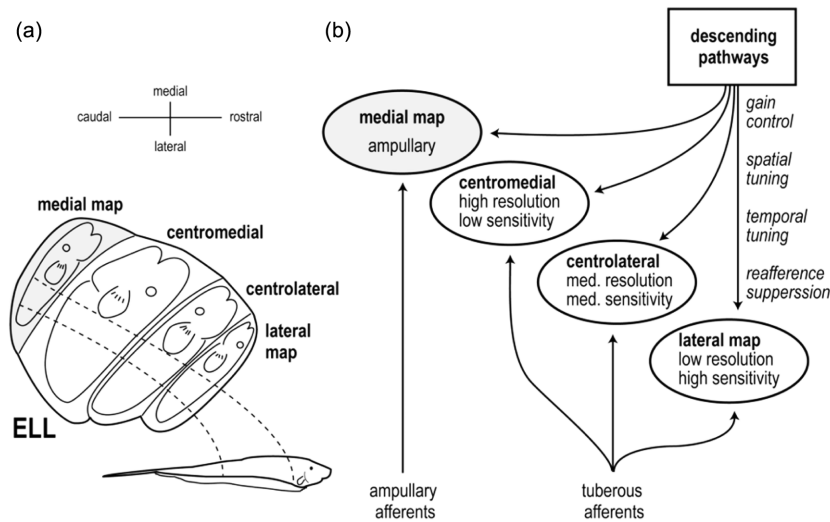
Fig. 4 The *ELL* can be viewed as an adaptive, multi-scale array of virtual smart sensors. (a) Illustration of the right *ELL* showing four topographic maps of passive (gray) and active (unshaded) electrosensory input. Modified from Heiligenberg and Dye (1982) and (b) principal neurons in each map process the primary afferent input with differing spatial, temporal and sensitivity characteristics. Descending signals provide gain control, frequency tuning, and suppression of background noise. From Nelson (2005)

own topographic map of the electroreceptive periphery. The medial map is devoted to processing information from the passive electric sense, which detects low frequency electric fields of extrinsic origin. The three lateral maps are devoted to the active electric sense based on the fish's own electric organ discharge. Each active electrosensory afferent nerve fiber trifurcates as it reaches the *ELL*, providing each of the three active maps with essentially identical input. The three maps are denoted by their anatomical locations as *CMS* (centromedial segment), *CLS* (centrolateral segment) and *LS* (lateral segment).

The *ELL* principal neurons filter the incoming electrosensory image data with spatiotemporal filtering properties that vary across the different maps (Krahe *et al.* 2008, Shumway 1989b). In comparison to the approximately 7,500 *P*-type afferents on each side of the body, there are approximately 2800 principal neurons in the *CMS* map, 1400 principal neurons in *CLS*, and 900 in *LS* (Maler 2009). The principal neurons in these three maps can be viewed as virtual sensors with spatial and temporal filtering properties that are unique to each map. The *LS* map, with only 900 principal neurons, has the highest degree of convergence from skin electroreceptors, with each principal neuron receiving input from approximately 1000 afferents. By performing extensive spatial averaging, the *LS* map exhibits the best sensitivity to weak stimuli, but has relatively poor spatial resolution. In contrast, the *CMS* segment, with 2800 principal neurons, has much less spatial convergence (only about 40 afferents per principal neuron) and thus has good spatial resolution but relatively low sensitivity to weak signals. The *CLS* segment has spatial convergence properties that are intermediate between *CMS* and *LS*.

The temporal filtering properties also vary across the three *ELL* segments. The *CMS* segment, which does very little spatial integration, does the most temporal integration, and thus has low-pass filtering characteristics (Krahe *et al.* 2008, Shumway 1989b). In contrasts, the *LS* segment, which does the most spatial integration, does very little integration in the time domain; thus *LS* principal

neurons retain the high-pass filtering characteristics of the *P*-type afferents. Again the CLS segment has properties intermediate between *CMS* and *LS*.

These tradeoffs in spatiotemporal integration across the three *ELL* segments can be understood as different strategies for optimizing signal-to-noise performance. Because the sensors are noisy, the fish can improve signal-to-noise by signal averaging, either in space, or in time, or both. The *LS* segment primarily implements spatial averaging, with little temporal averaging; the *CMS* segment implements temporal averaging with little spatial averaging; the *CLS* segment falls in the middle. With this multi-scale design, the system can implement different spatiotemporal filtering strategies for different situations depending on the nature of the task.

4.2 Sparse coding of stimulus features

Sparse coding in neural systems refers to an encoding in which a relatively small subset of neurons is active. Sparseness can be implemented in both space and time. In the spatial domain, it refers to relatively few neurons in a population being active; in the temporal domain, it refers to activity during a relatively few number of time windows. Sparse coding efficiently represents complex, dynamic stimuli utilizing a small number of active neurons, thus providing an energy-efficient and computationally fast method for encoding the signal structure (Gabbiani *et al*. 1996, Olshausen and Field 2004).

In the electrosensory system of weakly electric fish, single *P*-type electroreceptor afferents accurately encode the time course of modulations in transdermal potential amplitude across the behaviorally relevant bandwidth (Gabbiani *et al*. 1996). To do so, they generate spikes at relatively high rates, typically around 300 spikes/s. If we consider that there are approximately 7,500 *P*-type afferents on one side of the body, each firing at this rate, the total input spike rate to one side of the *ELL* is about 2×10^6 spikes/s. In contrast, the output spike rate of an *ELL* map segment is approximately two orders of magnitude lower. For example, the *LS* segment of the *ELL* contains 900 principal neurons, each firing at a rate of about 20 spikes/s (Krahe *et al*. 2008). So the total output spike rate from the *LS* map is only 2×10^4, compared to an input spike rate of 2×10^6. Thus the *ELL* output representation is sparse compared to the input representation.

The *ELL* principal neurons do not accurately encode the full time course of the stimulus. Instead they encode particular temporal features (such as rapid up-strokes and down-strokes) that are relevant to task performance. Thus *P*-type afferents appear to be specialized for accurately encoding the full stimulus waveform, whereas subsequent stages of neural processing appear to be specialized for extracting behaviorally relevant stimulus features. This trend from accurate encoding in the periphery to increasingly sparse representations of specific features seems to hold for several stages of electrosensory processing (Carlson and Kawasaki 2008).

4.3 Task-dependent adaptive filtering

The *ELL* receives extensive descending input from higher brain centers. Descending input exceeds primary afferent input by more than an order of magnitude in terms of the number of synapses received by each *ELL* principal neuron. These descending pathways carry a variety of contextual information and control signals that are useful for adaptive signal processing. These include electrosensory feedback signals, sensory signals from other modalities, proprioceptive signals related to body posture, and efference copy signals related to outgoing motor commands (Berman and Maler 1999). As shown in Fig. 4(b), the *ELL* can thus be visualized as a bank of adaptive spatiotemporal filters

that receive descending control signals. Each filter bank contains a topographically organized array of principal neurons that can be tuned and adjusted for particular tasks in particular contexts to optimize performance. For example, prey-related signals and communications-related signals evoke different frequency tuning and spike-timing properties in *ELL* principal neurons (Chacron *et al.* 2003). Prey-related electrolocation signals tend to be more localized on the receptor array than communications-related signals which mediate social interactions between weakly electric fish. Feedback pathways in the *ELL* dynamically regulate the flow of information through the system in these two contexts, resulting in the optimal encoding of both stimulus categories (Chacron *et al*. 2003).

4.4 Generation and subtraction of sensory expectation

A number of studies have demonstrated that the neural circuitry of the *ELL* also plays an important role in suppressing certain "expected" components of incoming electrosensory information (Bastian 1995, Bell 2001). Sensory reafference is a term used to describe the change in afferent activity that occurs due to an animal's own movements or actions. The *ELL* implements a reafference-suppression mechanism that is responsible for reducing background noise in wave-type electric fish associated with tail-bending movements that reposition the electric organ relative to the sensor array (Bastian 1995, Bastian *et al*. 2004). When the fish bends its tail to the left, the electric organ moves closer to the sensors on the left side of the body and causes an increase in spiking activity for those afferents. At the same time, electrosensory afferents on the right side of the body will exhibit a decrease in spiking activity. But the afferents on each side of the body are not all modulated to the same degree. The amount of modulation will depend on the precise location of the sensor along the body axis. The circuitry of the *ELL* adaptively cancels out this reafferent noise on a sensor-by-sensor basis. Descending signals to the *ELL* carry sensory information about the fish's trunk and body position. This information is passed to each principal neuron in the *ELL*. Using a biological equivalent of the least mean squares (*LMS*) adaptive filter algorithm that in used in engineering applications (Haykin 2002), each *ELL* principal neuron constructs a "negative image" of the expected pattern of sensory input. The negative image is formed by a correlation-based learning mechanism operating at descending pathway synapses and is built up over a period of several minutes. The adaptive reafference-suppression algorithm essentially filters out any components of the incoming sensory data stream that are consistently correlated with the animal's own movements over that time frame.

5. Conclusions

Weakly electric fish implement a number of sensory acquisition strategies that may provide useful guidance for the design of smart sensing systems in engineering applications. Using a self-generated electric field, the fish are able to detect, localize, and characterize sensory targets in complete darkness based on the analysis of dynamic electrosensory images. The electrosensory system accomplishes its task using an array of noisy, low-resolution sensors distributed across the body surface. To improve resolution at the system level, the fish oversamples the signal in both space and time using relatively large numbers of sensors and high sampling rates. Data from the electrosensory array are efficiently encoded into digital spike trains and subsequently processed in the central nervous system by parallel banks of adaptive, multi-scale, virtual sensor arrays with adjustable spatiotemporal filtering properties.

The choice of sensory system architecture and particular set of information-processing algorithms implemented by the fish can be viewed as optimizations that have been carried out via natural selection over evolutionary time scales. The evolutionary process explores the design space and arrives at solutions that implicitly take into account the various costs (e.g., metabolic load), constraints (e.g., biophysical limitations), and performance measures (e.g., prey-capture efficiency) that impact the animal's fitness in the context of its natural environment. Engineering applications will have their own sets of costs, constraints, and performance criteria, so biological solutions should not simply be copied or imitated. Instead, biological sensory systems should be analyzed from a reverse-engineering perspective to gain insight into the fundamental mechanisms and principles. These principles can then be incorporated the engineering design process to hopefully arrive at novel, bio-inspired solutions that outperform more traditional approaches in terms of overall robustness, reliability and efficiency.

Acknowledgements

References

Bastian, J. (1995), "Pyramidal-cell plasticity in weakly electric fish: a mechanism for attenuating responses to reafferent electrosensory inputs", *J. Comp. Physiol. A*, **176**(1), 63-78.

Bastian, J., Chacron, M.J. and Maler, L. (2004), "Plastic and nonplastic pyramidal cells perform unique roles in a network capable of adaptive redundancy reduction", *Neuron*, **41**(5), 767-779.

Bell, C.C. (2001), "Memory-based expectations in electrosensory systems", Curr. Opin. Neurobiol. 11, 481-487.

Berman, N.J. and Maler, L. (1999), "Neural architecture of the electrosensory lateral line lobe: adaptations for coincidence detection, a sensory searchlight and frequency-dependent adaptive filtering", *J. Exp. Biol.*, **202**, 1243-1253.

Brandman, R. and Nelson, M.E. (2002), "A simple model of long-term spike train regularization", *Neural Comput.*, **14**, 1575-1597.

Carlson, B.A. and Kawasaki, M. (2008), "From stimulus estimation to combination sensitivity: encoding and processing of amplitude and timing information in parallel, convergent sensory pathways", *J. Comput. Neurosci.*, **25**, 1-24.

Carr, C.E., Maler, L. and Sas, E. (1982), "Peripheral organization and central projections of the electrosensory nerves in gymnotiform fish", *J. Comp. Neurol.*, **211**(2), 139-153.

Chacron, M.J., Doiron, B., Maler, L., Longtin, A. and Bastian, J. (2003), "Non-classical receptive field mediates switch in a sensory neuron's frequency tuning", *Nature*, 423, 77-81.

Chen, L., House, J. H., Krahe, R. and Nelson, M.E. (2005), "Modeling signal and background components of electrosensory scenes", *J. Comp. Physiol. A*, **191**(4), 331-345.

Gabbiani, F., Metzner, W. and Wessel, R. and Koch, C. (1996), "From stimulus encoding to feature extraction in weakly electric fish", *Nature*, 284, 564-567.

Haykin, S. (2002), Adaptive Filter Theory, 4th Ed., Prentice Hall, Upper Saddle River, NJ. Heiligenberg, W. (1977), "Principles of electrolocation and jamming avoidance", In: Studies of Brain Function, **1**, (Ed. V. Braitenberg), Springer-Verlag, Berlin.

Hopkins, C.D. (1976), "Stimulus filtering and electroreception: tuberous receptors in three species of gymnotoid fish", *J. Comp. Physiol. A*, **111**(2), 171-207.

Kay, S.M. (1993), Fundamentals of Statistical Signal Processing: Estimation Theory, Prentice Hall, Upper Saddle River, NJ.

Knudsen, E.I. (1975), "Spatial aspects of the electric fields generated by weakly electric fish", *J. Comp. Physiol.*, **99**(2), 103-118.

Krahe, R., Bastian, J. and Chacron, M.J. (2008), "Temporal processing across multiple topographic maps in the electrosensory system", *J. Neurophysiol.*, **100**, 852-867.

Maler, L. (2009), "Receptive field organization across multiple electrosensory maps-I. Columnar organization and estimation of receptive field size", *J Comp. Neurol.*, **516**(5), 376-393

Nelson, M.E. (2005), "Target Detection, Image Analysis and Modeling", In: Electroreception (Springer Handbook of Auditory Research), (Eds. T.H. Bullock, C.D. Hopkins, A.N Popper, R.R. Fay), Springer, New York, 290-317.

Nelson, M.E. and MacIver, M.A. (1999), "Prey capture in the weakly electric fish Apteronotus albifrons: sensory acquisition strategies and electrosensory consequences", *J. Exp. Biol.*, **202**, 1195-1203.

Nelson, M.E. and MacIver, M.A. (2006), "Sensory acquisition in active sensing systems", *J. Comp. Physiol. A*, **192**(6), 573-586.

Nelson, M.E., Xu, Z. and Payne, J.R. (1997), "Characterization and modeling of P-type electrosensory afferent responses to amplitude modulations in a wave-type electric fish", *J. Comp. Physiol. A*, **181**(5), 532-544.

Olshausen, B.A. and Field, D.J. (2004), "Sparse coding of sensory inputs", *Curr. Opin. Neurobiol.*, **14**(4), 481-487.

Ratnam, R. and Nelson, M.E. (2000), "Nonrenewal statistics of electrosensory afferent spike trains: Implications for the detection of weak sensory signals", *J. Neurosci.*, **20**, 6672-6683.

Shumway, C.A. (1989a), "Multiple electrosensory maps in the medulla of weakly electric Gymnotiform fish I. Physiological differences", *J. Neurosci.*, **9**(12), 4388-4399.

Shumway, C.A. (1989b), "Multiple electrosensory maps in the medulla of weakly electric Gymnotiform fish II. Anatomical differences", *J. Neurosci.*, **9**(12), 4400-4415.

Xu, Z., Payne, J.R. and Nelson, M.E. (1996), "Logarithmic time course of sensory adaptation in electrosensory afferent nerve fibers in a weakly electric fish", *J. Neurophysiol.*, **76**(3), 2020-2032.